Journal of the American College of Cardiology
© 2013 by the American College of Cardiology Foundation
Published by Elsevier Inc.

Vol. 62, No. 9, 2013
ISSN 0735-1097/$36.00
http://dx.doi.org/10.1016/j.jacc.2013.03.081

Inverse Relationship Between Fractionated Electrograms and Atrial Fibrosis in Persistent Atrial Fibrillation

Combined Magnetic Resonance Imaging and High-Density Mapping

Amir S. Jadidi, MD,*† Hubert Cochet, MD,* Ashok J. Shah, MD,* Steven J. Kim, MEEng,‡ Edward Duncan, MD,* Shinsuke Miyazaki, MD,* Maxime Sermesant, PhD,§ Heiko Lehrmann, MD,† Matthieu Lederlin, MD,* Nick Linton, MEng,* Andrei Forclaz, MD,* Isabelle Nault, MD,* Lena Rivard, MD,* Matthew Wright, MBBS,* Xingpeng Liu, MD,* Daniel Scherr, MD,* Stephen B. Wilton, MD,* Laurent Roten, MD,* Patrizio Pascale, MD,* Nicolas Derval, MD,* Frédéric Sacher, MD,* Sebastien Knecht, MD,* Cornelius Keyl, MD,† Mélèze Hocini, MD,* Michel Montaudon, MD,* Francois Laurent, MD,* Michel Haïssaguerre, MD,* Pierre Jaïs, MD*

Bordeaux and Sophia-Antipolis, France; Bad Krozingen, Germany; and St. Paul, Minnesota

Objectives This study sought to evaluate the relationship between fibrosis imaged by delayed-enhancement (DE) magnetic resonance imaging (MRI) and atrial electrograms (Egms) in persistent atrial fibrillation (AF).

Background Atrial fractionated Egms are strongly related to slow anisotropic conduction. Their relationship to atrial fibrosis has not yet been investigated.

Methods Atrial high-resolution MRI of 18 patients with persistent AF (11 long-lasting persistent AF) was registered with mapping geometry (NavX electro-anatomical system (version 8.0, St. Jude Medical, St. Paul, Minnesota)). DE areas were categorized as dense or patchy, depending on their DE content. Left atrial Egms during AF were acquired using a high-density, 20-pole catheter (514 ± 77 sites/map). Fractionation, organization/regularity, local mean cycle length (CL), and voltage were analyzed with regard to DE.

Results Patients with long-lasting persistent versus persistent AF had larger left atrial (LA) surface area (134 ± 38 cm^2 vs. 98 ± 9 cm^2, $p = 0.02$), a higher amount of atrial DE (70 ± 16 cm^2 vs. 49 ± 10 cm^2, $p = 0.01$), more complex fractionated atrial Egm (CFAE) extent (54 ± 16 cm^2 vs. 28 ± 15 cm^2, $p = 0.02$), and a shorter baseline AF CL (147 ± 10 ms vs. 182 ± 14 ms, $p = 0.01$). Continuous CFAE (CFEmean [NavX algorithm that quantifies Egm fractionation] <80 ms) occupied 38 ± 19% of total LA surface area. Dense DE was detected at the left posterior left atrium. In contrast, the right posterior left atrium contained predominantly patchy DE. Most CFAE (48 ± 14%) occurred at non-DE LA sites, followed by 41 ± 12% CFAE at patchy DE and 11 ± 6% at dense DE regions ($p = 0.005$ and $p = 0.008$, respectively); 19 ± 6% CFAE sites occurred at border zones of dense DE. Egms were less fractionated, with longer CL and lower voltage at dense DE versus non-DE regions: CFEmean: 97 ms versus 76 ms, $p < 0.0001$; local CL: 153 ms versus 143 ms, $p < 0.0001$; mean voltage: 0.63 mV versus 0.86 mV, $p < 0.0001$.

Conclusions Atrial fibrosis as defined by DE MRI is associated with slower and more organized electrical activity but with lower voltage than healthy atrial areas. Ninety percent of continuous CFAE sites occur at non-DE and patchy DE LA sites. These findings are important when choosing the ablation strategy in persistent AF. (J Am Coll Cardiol 2013;62:802–12) © 2013 by the American College of Cardiology Foundation

From the *Hôpital Cardiologique du Haut-Lévêque and the Université Victor Segalen Bordeaux II, Bordeaux, France; †Universitaets-Herzzentrum Freiburg-Bad Krozingen, Bad Krozingen, Germany; ‡St. Jude Medical, St. Paul, Minnesota; and the §INRIA, Asklepios Project, Sophia-Antipolis, France. The research leading to these results was funded by the European Union Seventh Framework Programme (FP7/2007-2013) under grant agreement HEALTH-F2-2010-261057. Dr. Jadidi has received a research grant from Hopitaux Universitaire de Geneve and St. Jude Medical. Dr. Wilton has received a research grant from St. Jude Medical. Dr. Jais has received consulting fees and honoraria from St. Jude Medical and Biosense Webster. All other authors have reported that they have no relationships relevant to the contents of this paper to disclose.

Manuscript received December 18, 2012; revised manuscript received March 19, 2013, accepted March 24, 2013.

Atrial fibrillation (AF) is the most common arrhythmia associated with substantial morbidity/mortality in humans. The pulmonary veins (PVs) are the main drivers of paroxysmal AF, and their isolation by ablation is associated with restoration of sinus rhythm (1). In persistent and long-persistent AF, PVs play a less prominent role than widespread structural and functional alterations in the atrial substrate, which lower the success rate of pulmonary vein isolation (PVI) alone. Therefore, ablation strategies targeting complex fractionated atrial electrogram (CFAE) sites in addition to PVI have been shown to improve maintenance of sinus rhythm (2,3). CFAEs are associated with slow anisotropic conduction in experimental conditions (4–6). They may also result from far-field signals arising from adjacent myocardium (double counting) or from wave collision during AF (7,8) or rapid focal or re-entrant activity (9), preferentially at ganglionated plexus sites (10).

See page 813

Histopathological studies in humans and canine models of persistent AF have reported extracellular matrix remodeling with fibrotic infiltration causing atrial dilation (11,12). Studies using gadolinium-enhanced magnetic resonance imaging (MRI) have described areas of delayed enhancement (DE) in the atrial wall of patients with AF due to the presence of fibrosis. Recent clinical studies suggest that a high burden of atrial DE (aDE) before ablation might be associated with poor post-ablation outcome (13). This may be related to the impact of fibrosis on wave propagation during AF (12). We assessed the role of atrial fibrosis on the characteristics of atrial electrograms (Egms) during AF.

Methods

Patients. We prospectively enrolled 18 consecutive patients referred to our center between June and September 2010 for ablation of persistent AF. Our institutional review board approved the study, and each of the patients provided a written informed consent. Inclusion criteria were the presence of persistent (lasting >7 days) or long-persistent (lasting >12 months) AF without a history of ablation. Exclusion criteria were contraindications to MRI (e.g., metal implants, claustrophobia) and the presence of atrial thrombi on pre-procedural transesophageal echocardiography. Among 18 patients (mean age, 63 ± 7 years; range, 47 to 70 years; 2 women), 11 had long-lasting persistent AF. Antiarrhythmic medications were discontinued for 5 half-lives before the ablation procedure. All patients underwent cardiac MRI 1 to 2 days before the procedure. High-density left atrial (LA) mapping was performed during AF before ablation.

Magnetic resonance imaging. IMAGE ACQUISITION. MRI studies were conducted on a 1.5-T clinical scanner (Avanto, Siemens Medical Solutions, Erlangen, Germany) equipped with a 32-channel cardiac coil. DE MRI was performed 15 min after the administration of 0.2 mmol/kg gadoterate dimeglumine (Dotarem, Guerbet, France). Imaging was acquired with the use of a 3-dimensional, inversion recovery–prepared, respiration-navigated, ECG-gated, gradient-echo pulse sequence with fat-saturation. ECG gating was set to 50% of the mean RR interval to acquire signal in mid-diastole. Acquisition parameters were as follows: voxel size, 1.25 × 1.25 × 2.5 mm (reconstructed to 0.625 × 0.625 × 2.5 mm with in-plane interpolation); flip angle, 22°; repetition time/echo time, 5.4/2.3 ms; inversion time, 260 to 320 ms (depending on the results of a previously acquired TI scouting sequence); parallel imaging with GRAPPA technique $R = 2$; and number of reference lines, 44. Scan time ranged 5 to 10 min depending on the patient's heart and respiratory rates.

Abbreviations and Acronyms

aDE = atrial delayed enhancement
AF = atrial fibrillation
CFAE = complex fractionated atrial electrogram
CFEmean = NavX algorithm that quantifies electrogram fractionation
CL = cycle length
CS = coronary sinus
DE = delayed enhancement
Egm = electrogram
LA = left atrial
MRI = magnetic resonance imaging
PV = pulmonary vein
PVI = pulmonary vein isolation

Image post-processing. Image post-processing was performed by 2 observers (H.C., S.K.). Image processing was performed before the electrophysiology (EP) procedure, and the observer was blinded to all EP data. Segmentation was performed with OsiriX 3.6.1 (OsiriX Foundation, Geneva, Switzerland). For modeling we used CardioViz3D (INRIA, Sophia Antipolis, France). LA was segmented manually by contouring the endocardial and epicardial borders of the atrium, including the PV ostia and the first 2 cm of each PV. Areas of aDE were detected and segmented by performing a slice-by-slice histogram analysis with a semiautomatic signal threshold, as described previously (13) (for details, see Fig. 1). From the segmented images, the LA blood pool volume was quantified (corresponding to LA endocardial volume). Two series of binary images were produced for modeling purposes: the first one corresponding to the areas of aDE and the second one corresponding to the blood pool volume, including PVs and coronary sinus to provide landmarks for subsequent registration with the NavX LA geometry. Three-dimensional meshes of LA blood pool volume and aDE volumes were computed using CardioViz3D (INRIA, Sophia Antipolis, France) and exported as XML into the NavX system (St. Jude Medical, St. Paul, Minnesota). DE LA sites were differentiated into: 1) dense/continuous DE regions; and 2) patchy/intermittent DE regions if the DE was noncontinuous and nonenhanced tissue was found in between the DE sites. We considered atrial tissue as dense/continuously enhanced if >90% of that regional atrial surface area contained DE. Patchy/intermittent DE was defined as inhomogeneous infiltration of atrial tissue by DE (DE

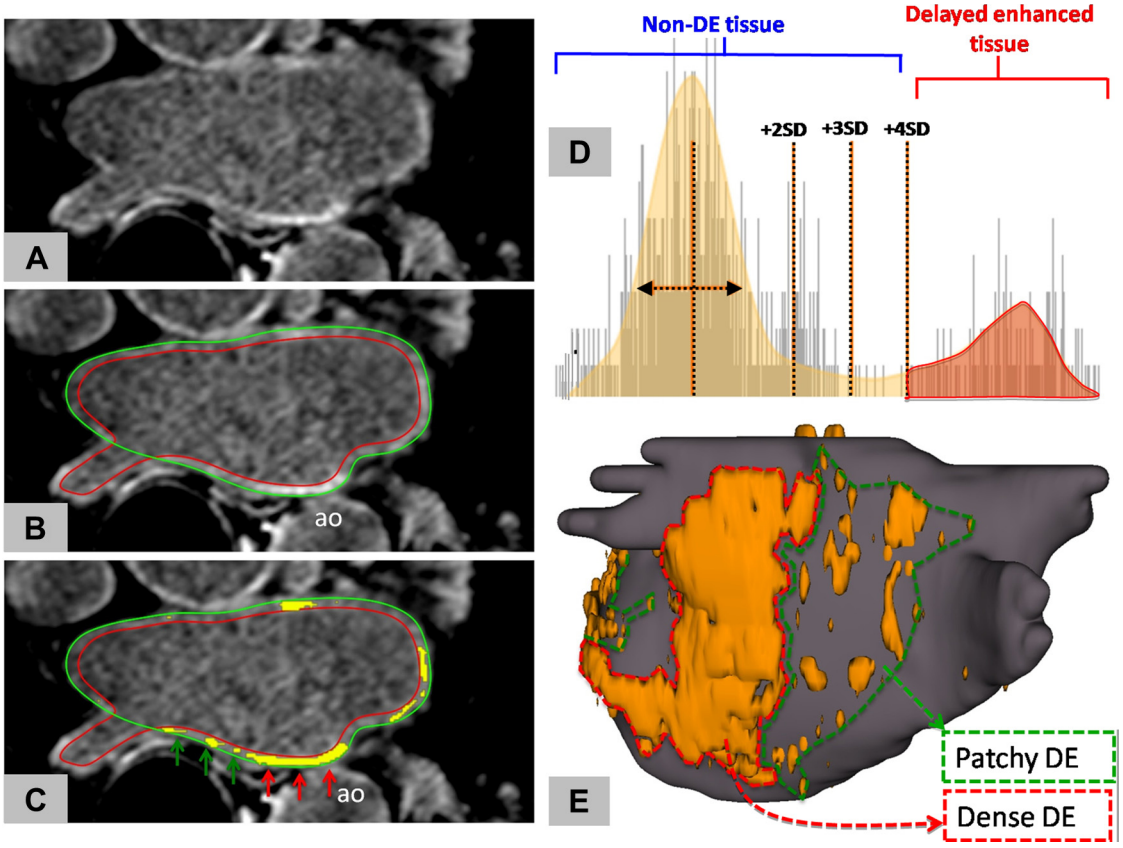

Figure 1 Detection, Segmentation, and 3-Dimensional Reconstruction of Atrial DE

(A) High-resolution (1.25 × 1.25 × 2.5 mm) delayed enhancement (DE) magnetic resonance imaging. **(B)** Segmentation of the left atrial wall between the inner **(red)** and outer **(green)** markers. **(D)** Voxel intensity histogram analysis of left atrial wall identifies DE as voxel intensities >4 SD than the mean in-plane voxel intensity. **(C)** Regions of DE are depicted in **yellow**. **(E)** Three-dimensional (3D) reconstruction of left atrial blood pool and DE areas. Dense DE regions are measured using the **red marker in E** with corresponding **red arrows in C**, and patchy DE regions are measured using the **green marker in E** with corresponding **green arrows in C**. ao = descending aorta.

content 20% to 70% of regional surface area). If the atrial tissue did not contain any DE on MRI, it was qualified as non-DE area (Figs. 1 and 2).

AF cycle length at baseline. In each patient, the baseline AF cycle length (CL) was measured in the LA appendage (LAA) over 20 AF cycles during CFAE mapping.

Electrophysiological mapping. CO-REGISTRATION OF MRI AND ELECTROPHYSIOLOGICAL DATA. After establishing transseptal access to LA, 50 IU/kg heparin was given intravenously. LA geometry was acquired using a double-loop 20-pole catheter AFocus II HD (St. Jude Medical). The LA geometry was carefully registered with the LA blood pool volume derived from MRI. This process was achieved by performing a point-by-point registration of 40 to 50 anatomic landmarks (PVs, LAA, and coronary sinus vein [CS]) (Fig. 2). A decapolar catheter (Xtrem, ELA Medical, Montrouge, France) was used as spatial reference.

Mapping of CFAE and analysis of surface areas with continuous CFAE vis-à-vis DE. CFAE maps were acquired using a 20-pole catheter (AFocus II HD, St. Jude Medical, St. Paul, Minnesota) and the NavX electroanatomical system (version 8.0, St. Jude Medical). Bipolar Egms were filtered at 30 to 300 Hz and analyzed to compute mean fractionation (CFEmean map) and bipolar voltage during an 8-s recording period at each site. For optimal detection of continuous CFAE using a NavX CFEmean algorithm: minimum peak-to-peak Egm voltage for detection was set at 0.08 mV with a refractory period setting of interval detection of 40 ms (8,14). Continuous CFAE sites were defined as sites with CFEmean interval <80 ms (8), which, in our experience, corresponds to the continuous CFAE sites that are targeted for ablation (15). Spatial relationships between continuous CFAE and the regions of aDE were quantified by manually contouring both areas, as well as the region of overlap (between continuous CFAE and dense DE and continuous CFAE and patchy DE), on the registered volume. Each of these surface areas was measured separately and expressed as a percentage of the total LA area, total CFAE area, total dense DE area, and total patchy DE area.

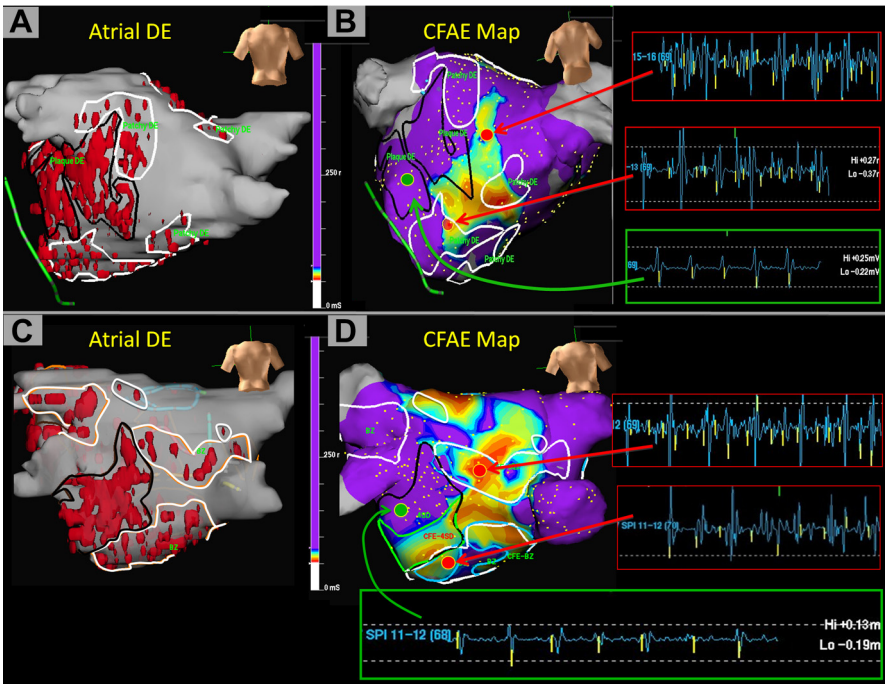

Figure 2 **Relationship of Atrial DE to Continuous CFAE Sites**

Examples showing relationship between dense delayed enhancement (DE), patchy DE, and continuous complex fractionated atrial electrogram (CFAE) sites (CFEmean [NavX algorithm that quantifies electrogram fractionation] <80 ms) from 2 patients with long-lasting persistent atrial fibrillation. Spatial distribution of dense DE **(black-marked areas)** and patchy DE after 3-dimensional reconstruction of MRI data (posterior view) **(A,C)**. Continuous CFAEs occupy 38 ± 19% of total left atrial surface. Most CFAEs (48 ± 14%) occur at non-DE areas followed by 41 ± 12% at patchy DE areas. A minority of CFAEs (11 ± 6%) occurs at dense DE areas. Dense DE areas display slower and more organized electrical activity than elsewhere (see electrograms in **green [B and D]**). Dense DE was found at the left posterior left atrium (LA), whereas patchy DE was frequently observed at the right posterior LA, LA roof, LA septum, and anterior LA wall. See accompanying Online Figures S1A to S1D.

Analysis of Egms of dense DE, patchy DE, and non-DE regions. For the analysis of Egm characteristics of dense DE versus patchy DE versus non-DE, we exported Egms from each of these regions from the CFAE maps. The exported Egms were analyzed according to their CFEmean value (8-s recording period), CL (1-s recording period), and mean voltage in AF (8-s recording period). For CL measurement, we analyzed the subset of organized Egms, where the local CL could be clearly identified (green Egms in Figs. 2B and 2D).

Quantification of organized Egms of dense DE versus patchy DE versus non-DE. Bipolar Egms were scrutinized and categorized into organized or nonorganized activity. Egms were considered nonorganized if fractionation led to the absence of an isoelectric baseline, making local CL measurement impossible at that site (red Egms in Figs. 2B and 2D). These nonorganized Egms were then temporarily removed from the map. The remaining organized Egms where the measurement of AF CL was feasible were compared with the total number of mapped Egms in that region.

The percentage of organized Egms per region = number of organized Egms/(number of organized Egms + number of nonorganized Egms) × 100. We calculated the percentage of Egms with organized activity at LA sites with DE versus patchy DE versus non-DE.

AF ablation. Irrigated RF ablation (Thermocool, Biosense Webster, California) applied 25 W on the posterior LA and 28 W on the LA roof and anterior PV antrum. Patients with persistent AF (>7 days) underwent proximal PVI followed by electrical cardioversion, if AF persisted and linear lesions if atrial flutter was obtained.

Patients with long-persistent AF underwent stepwise ablation. PVI was followed by ablation of continuous CFAE (CFEmean <80 ms) in the following order: LA roof, septum, inferior LA (facing the CS), lateral LA wall (at mitral isthmus region), and base of the LAA. CFAE at anterior LA were targeted before CFAE within the CS and at the posterior LA. The CLs within the left and right atrial appendages were measured after each ablation step. If right atrial appendage CL was shorter by >10 mm than the LAA CL, further CFAE ablation was performed at rapid fractionated sites within the right atrium. If AF did not terminate during CFAE ablation, linear ablation at the LA roof, lateral mitral isthmus including epicardial ablation within coronary sinus (at ≤25 W), and cavotricuspid isthmus was performed. If AF persisted, patients were cardioverted electrically, and PVI and bidirectional linear blocks were ascertained.

Statistical analysis. Statistical analysis was performed using SPSS for Windows version 16.0 (SPSS, Inc., Chicago,

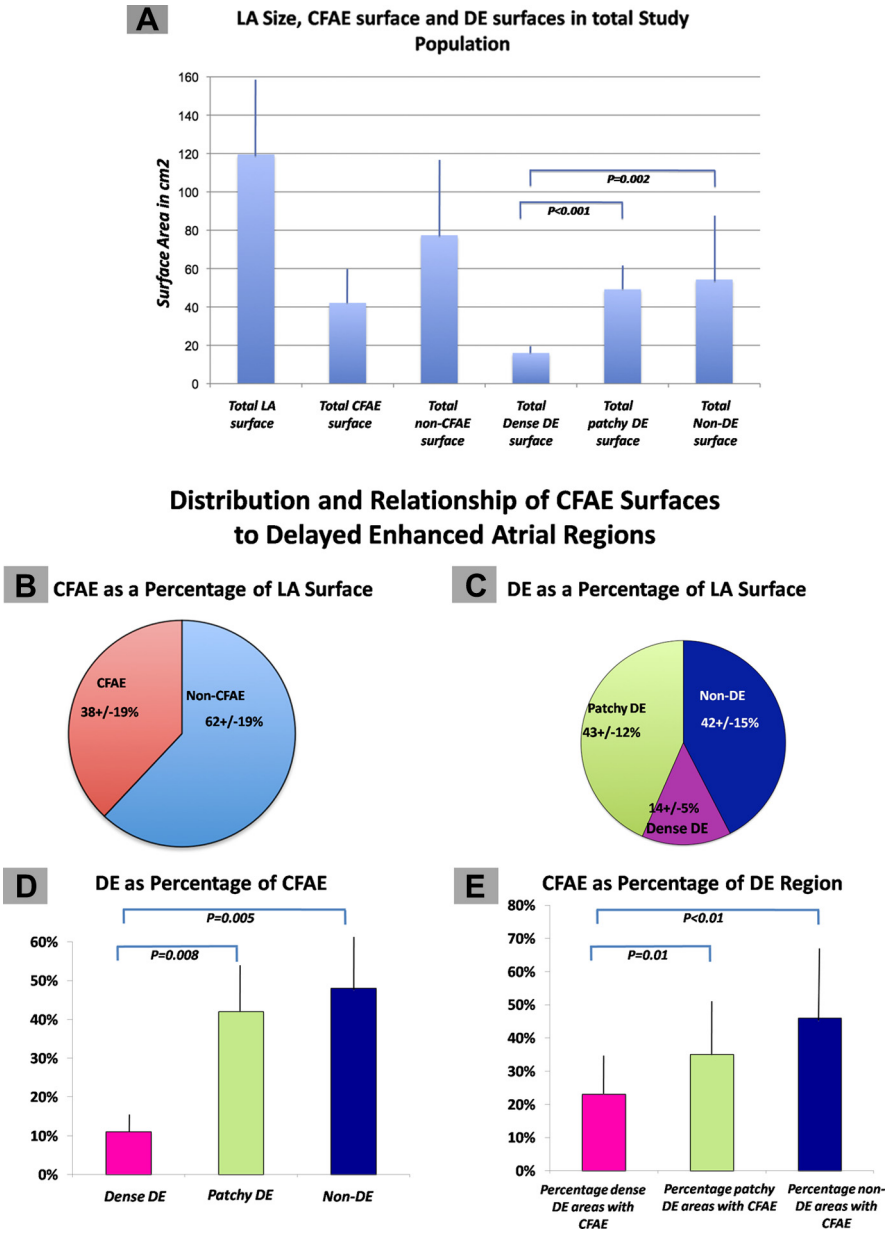

Figure 3 Total and Relative Distributions of CFAE Sites, Dense DE, Patchy DE and Non-DE Atrial Sites

(A) Quantitative assessment of left atrial (LA) size, extent of continuous complex fractionated atrial electrogram (CFAE), and atrial delayed enhancement (DE) regions. Distribution and relationship of CFAE surfaces to DE regions. **(B)** Continuous CFAE occupied 38 ± 19% of LA surface. **(C)** Dense DE took up 14 ± 5% and patchy DE took up 43 ± 12% of the LA surface. Most CFAEs (48 ± 14%) occurred at non-DE sites, followed by patchy (41 ± 12%) and dense (11 ± 6%) DE sites **(D)**. **(E)** CFAEs were displayed in 23 ± 13% of dense DE, 35 ± 18% of patchy DE, and 46 ± 27% of non-DE regions.

Illinois). Continuous data are presented as mean ± SD. In the absence of normal distribution, the nonparametric Mann-Whitney *U* test was used for comparing the groups. Because Egm characteristics (fractionation [CFE-mean], CL, and voltage) showed a positively skewed distribution, data were analyzed using nonparametric tests. The Kruskal-Wallis 1-way analysis of variance of ranks was performed to compare data for the 3 groups. Post-hoc analyses were carried out using the 2-sided Mann-Whitney *U* test. Categorical data were compared between different groups using the chi-square test. The Pearson correlation coefficient was used to calculate the correlation between the extent of DE and AF CL. Exponential line fitting was chosen based on the equation: $y = ax^b$. The median with the first and third quartiles (Q1, Q3) is reported for skewed data with asymmetrical distribution (Figs. 5A, 6A, and 6C).

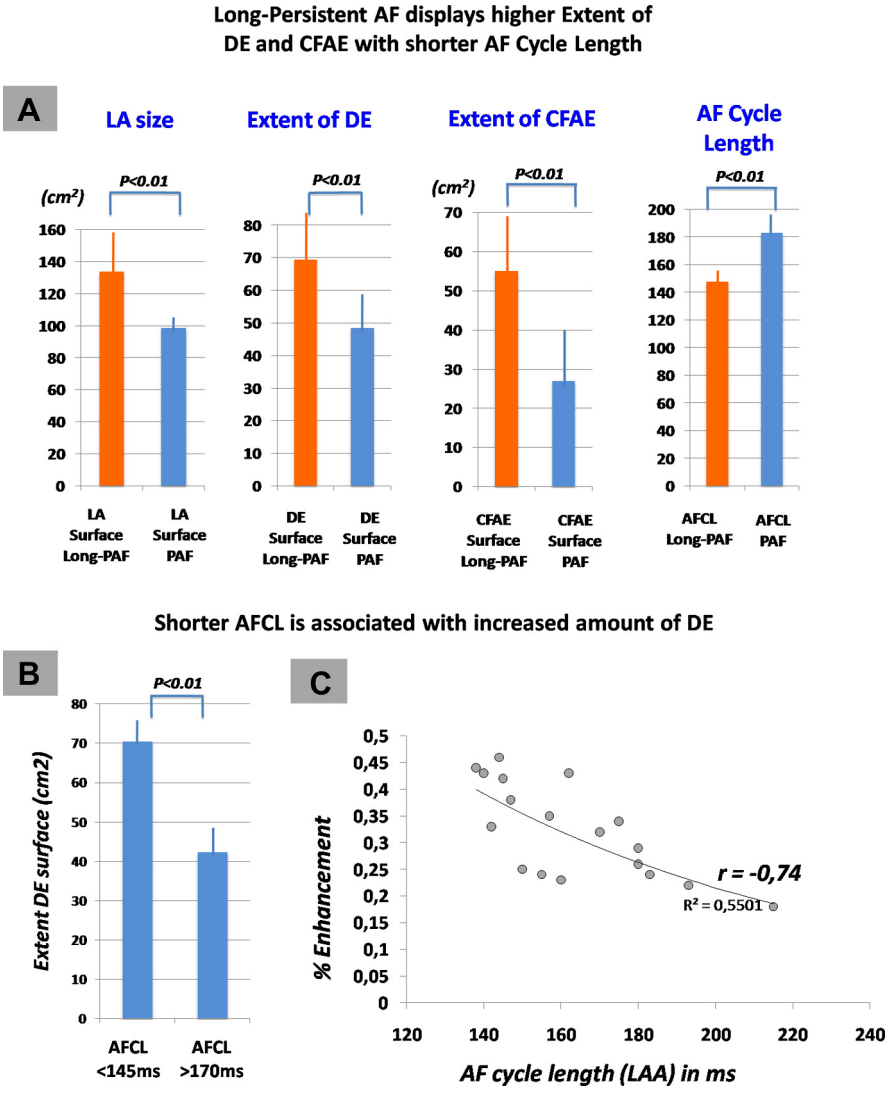

Figure 4 Relationship Between LA Size, Total Atrial DE, AF Cycle Length, and Extent of Continuous CFAEs in Patients With Long-Lasting Persistent and Persistent AF

(A) Long-persistent atrial fibrillation (AF) patients have larger LA size, higher extent of total atrial DE, larger extent of continuous CFAE regions, and shorter atrial fibrillation cycle length (AFCL). **(B)** Patients with shorter baseline AFCL have a greater extent of atrial DE. **(C)** An inverse correlation exists between the extent of atrial DE and AFCL. **Dots** represent values of single patients. LAA = left atrial appendage; PAF = persistent atrial fibrillation; other abbreviations as in Figure 3.

A p value <0.05 was considered statistically significant. The alpha error level was corrected to 0.016 for triplicate performance of the Mann-Whitney *U* test.

Results

Among 18 persistent AF patients, there were 11 with long-persistent AF.

High-density mapping of CFAE. The CFAE map density was 514 ± 77 sites/patient (range: 380 to 676; 2.93 ± 0.79 points/cm^2), amounting to 9,252 sites (Egms) recorded in 18 patients in total.

LA size, extent of aDE, and CFAE sites. STUDY POPULATION. Tables 1 and 2 show patient characteristics. The mean LA volume was 130 ± 31 ml, LA surface area was 119 ± 39 cm^2, and the AF CL within the LAA was 153 ± 15 ms. We considered atrial tissue as dense/continuously enhanced if >90% of the regional surface area showed DE on MRI. Patchy/intermittent DE was defined as inhomogeneous enhancement on MRI. The percentage of DE within the dense DE versus patchy DE areas was 96 ± 4% versus 37 ± 12%, respectively ($p < 0.0001$). Atrial regions without DE were considered non-DE areas (Figs. 1 and 2).

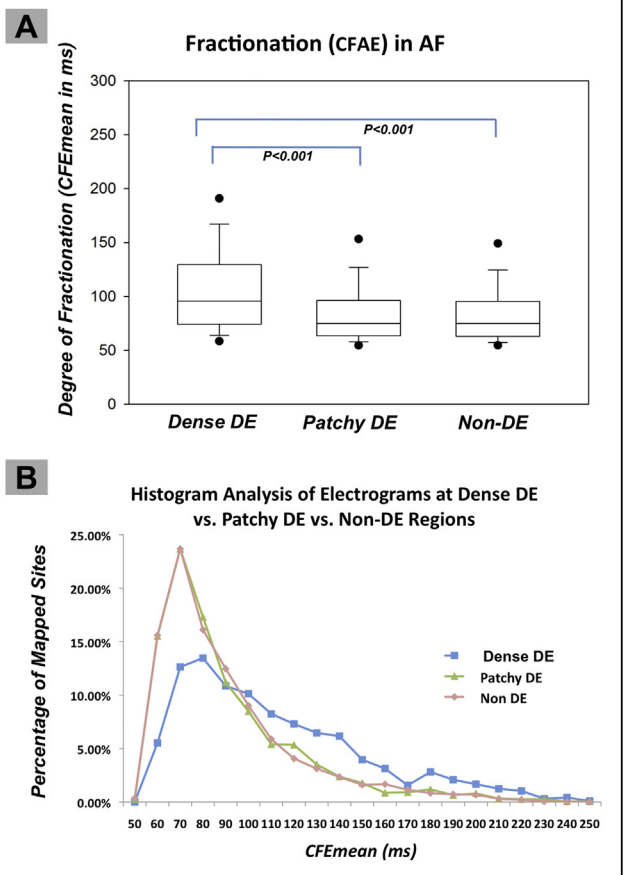

Figure 5 **Degree of Fractionation at Dense DE Versus Patchy DE Versus Non-DE Regions**

Degree of electrogram fractionation was lower with higher CFEmean (NavX algorithm that quantifies electrogram fractionation) intervals at dense DE (108 ± 44 ms; median: 97.1 ms) versus patchy DE (87 ± 34 ms; median, 75.8 ms, $p < 0.0001$) and non-DE sites (85.7 ± 32 ms; median, 75.8 ms, $p < 0.0001$ **[A]**). **(B)** Histogram analysis of CFEmean at dense DE versus patchy DE and non-DE regions. Continuous CFAE (CFEmean <80 ms) constituted ~57% of electrograms recorded within patchy DE or non-DE regions **(green and pink)** versus <33% in dense DE regions ($p = 0.009$ **[B]**). Abbreviations as in Figure 3.

In total, DE occupied 65 ± 13 cm^2 (57 ± 15%) and non-DE regions occupied 54 ± 33 cm^2 (42 ± 15%) of the LA area. The area of dense DE was smaller than that of the patchy DE: 16 ± 4 cm^2 (14 ± 5% of total LA surface) and 49 ± 13 cm^2 (43 ± 12% of total LA surface; $p < 0.001$, respectively) (Figs. 2A, 2C, 3A, and 3C).

The total surface area of continuous CFAE was 42 ± 18 cm^2 (38 ± 19% of LA surface (Fig. 3A).

DE surface areas and electrical parameters in long-persistent versus persistent AF. Patients with long-persistent AF had a larger LA surface area (134 ± 38 cm^2 vs. 98 ± 9 cm^2, $p = 0.02$), with a greater amount of total aDE (70 ± 16 cm^2 vs. 49 ± 10 cm^2, $p = 0.01$) and more continuous CFAE surface area (54 ± 16 cm^2 vs. 28 ± 15 cm^2, $p = 0.02$) (Fig. 4A) than persistent AF.

Although the extent of dense DE was similar in patients with long-persistent and persistent AF (16.9 ± 4 cm^2 vs. 16.6 ± 4.4 cm^2, $p = 0.88$), the extent of patchy DE was higher in patients with long-persistent AF (53 ± 14 cm^2 vs. 34 ± 9 cm^2, $p = 0.01$).

Dense DE was consistently encountered in all patients on the left side of the posterior left atrium adjacent to the left PV ostia and within the track/path of the descending aorta (Fig. 1C). The distribution of patchy DE was variable, although the right side of the posterior LA (toward the right PV ostia) showed patchy DE in all patients with long-persisting AF. Moreover patchy DE was frequently found at LA roof and the anteroseptal LA wall.

Baseline LA appendage AF CL was shorter in patients with long-persistent than persistent AF (147 ± 10 ms vs. 182 ± 14 ms, $p = 0.01$) (Fig. 4A). The patients with a very short AF CL (<145 ms) had a greater extent of total DE (71 ± 7 cm^2) than the patients with CL >175 ms (42 ± 5 cm^2, $p = 0.01$) (Fig. 4B). In general, AF CL and the extent of aDE were inversely correlated ($r = -0.74$) (Fig. 4C).

Analysis of the distribution of continuous CFAE vis-à-vis DE. Figure 3A illustrates the absolute surface areas of the left atrium, dense DE, patchy DE, non-DE, and continuous CFAE sites. Figures 3B to 3E illustrates the relative extent of CFAE and DE. Continuous CFAE sites occupied 38 ± 19% of the LA area (Figs. 3A and 3B). Dense and patchy DE occupied 14 ± 5% and 43 ± 12% of total LA surface, respectively; 42 ± 15% of LA surface did not show any DE (non-DE area) (Fig. 3C).

A minority of continuous CFAE sites occurred at dense DE regions (11 ± 6% of CFAE sites), whereas most of it (48 ± 14%) occurred at non-DE sites ($p = 0.005$), followed by 41 ± 12% at patchy DE regions ($p = 0.008$) (Figs. 2A to 2D and 3D). Notably, 19 ± 6% of CFAE sites occurred at border zones of dense DE or within dense DE regions.

A minority (23 ± 13%) of dense DE regions (4 ± 5% of the LA surface) displayed continuous CFAE (Figs. 2, 3E, and 5B). The majority of dense DE regions showed organized electrical activity. On the other hand, 35 ± 18% of patchy DE regions (15 ± 12% of LA surface) (Fig. 3E) and notably 46 ± 27% of non-DE regions displayed continuous CFAE (19 ± 8% of the LA surface) (Fig. 3E).

Egm fractionation (CFAE) at LA sites with dense DE versus patchy versus non-DE sites. Less Egm fractionation (with higher CFEmean values) was found at sites with dense DE (108 ± 44 mm) versus patchy DE (87 ± 34 mm, $p < 0.0001$) versus non-DE regions (85.7 ± 32 mm, $p < 0.0001$) (Fig. 5A). Notably, 57% and 56% of Egms within patchy DE (Fig. 5B, green curve) and non-DE regions (pink curve) displayed continuous CFAE (CFEmean <80 mm). In contrast, 33% of Egms within dense DE region showed continuous CFAE (Fig. 5B, blue curve) ($p = 0.009$).

Egm CL at LA sites with dense DE versus patchy DE versus non-DE. Dense DE areas showed slower and more organized electrical activity during AF than the other sites. The mean CL at sites with dense DE was 155 ± 28 ms

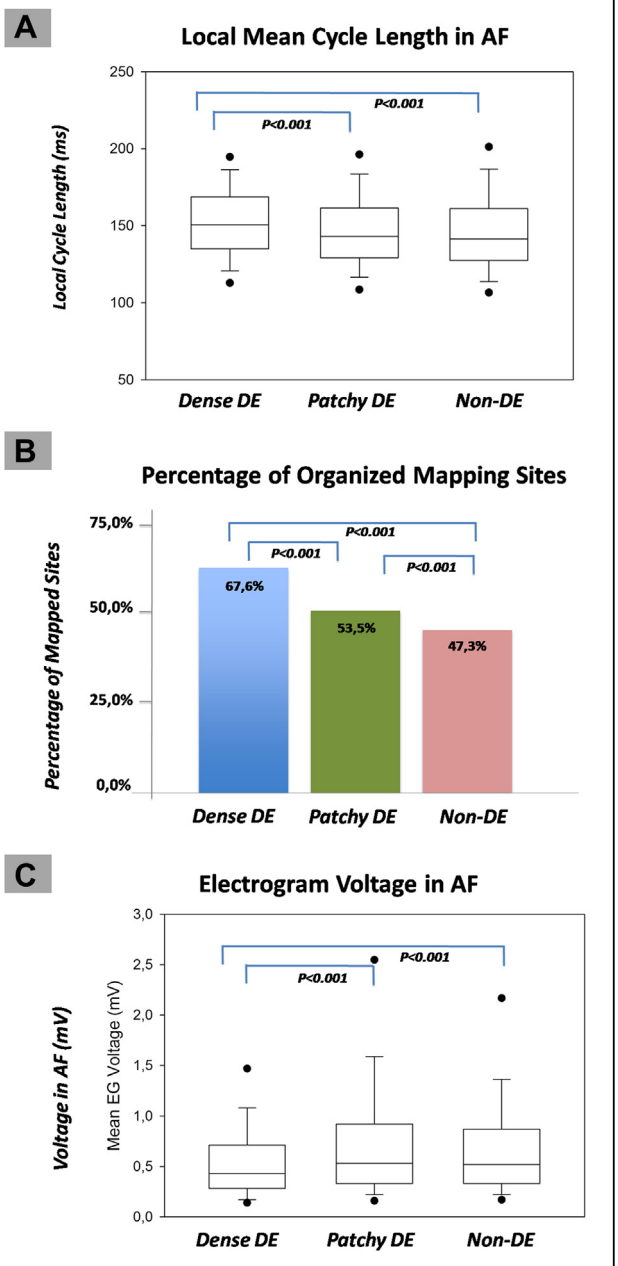

Figure 6 Electrogram Cycle Length, Organization, and Voltage Depend on Amount of Atrial Fibrosis (DE)

Electrogram cycle length **(A)**, organized activity **(B)**, and bipolar voltage **(C)** between dense DE versus patchy DE versus non-DE sites. Dense DE sites showed slower and more organized electrical activity with lower mean bipolar voltage during AF than other LA sites **(A to C)**. Abbreviations as in Figure 4.

versus 148.6 ± 28 ms at patchy DE ($p < 0.0001$) and 148.2 ± 29.3 ms at non-DE areas ($p < 0.0001$) (Fig. 6A). There was no difference in AF CL at patchy DE versus non-DE areas ($p = 0.92$).

Distribution of organized electrical activity at dense DE versus patchy DE versus non-DE regions. A total of 9,252 Egms were recorded among 18 patients included in the study (514 ± 77 per patient). After qualitative analysis by visual inspection of a 1-s recording period at each mapped site, 53.6% of all Egms were characterized as organized and 46.4% as nonorganized. Organized Egms were more

Table 1 Clinical Characteristics of Study Population (N = 18)

Age, yrs	63 ± 7
Male/female	16/2
History of AF, months	81 ± 65
Duration of continuous AF, months	25 ± 27
Long-persistent AF (>12 months)	11
LVEF, %	53 ± 13
Left ventricular dysfunction (LVEF <50%)	9
LVEDD, mm	54 ± 7
LVESD, mm	36 ± 9
IVSDD, mm	12 ± 2
LAD, mm	46 ± 7
Structural heart disease	7
Coronary artery disease	1
Hypertension	13
No. of failed AAD	2.4 ± 1.0
Administration of amiodarone	12
No. of electrical cardioversions	1.8 ± 0.8
Left atrial appendage cycle length, ms	153 ± 15

Values are mean ± SD or n.

AAD = antiarrhythmic drug; AF = atrial fibrillation; LVEDD = left ventricular end-diastolic diameter; LVEF = left ventricular ejection fraction; LVESD = left ventricular end-systolic diameter; IVSDD = interventricular septum diastolic diameter; LAD = left atrial diameter (anteroposterior).

Table 2 Comparison Characteristics in Patients With Persistent (>7 Days) and Long-Persistent (>12 Months of Continuous AF) AF

	Long-Persistent AF (n = 11)	Persistent AF (n = 7)	p Value
Age, yrs	64 ± 9	59 ± 8	0.13
Male/female	10/1	7/0	0.43
History of AF, months	86 ± 61	78 ± 71	0.90
Duration of continuous AF, months	25 ± 8	2 ± 1	**0.02**
LVEF, %	48 ± 11	57 ± 9	0.07
Total left atrial surface area, cm^2	134 ± 38	98 ± 9	**0.02**
Extent of atrial DE, cm^2	69.5 ± 15.6	48.5 ± 9.6	**0.01**
Extent of continuous CFAE, cm^2	54 ± 6	28 ± 15	**0.02**
Left ventricular dysfunction (<50%)	4	2	0.17
LVEDD	59 ± 6	55 ± 4	0.06
IVSDD	12 ± 1	11 ± 2	0.73
LAD, mm	49 ± 5	43 ± 4	0.06
Structural heart disease	6	1	0.08
Coronary disease	1	0	0.53
Hypertension	8	5	0.42
No. of failed AAD	2.1 ± 1.0	1.7 ± 1.0	0.38
Administration of amiodarone	10/11	6/7	0.52
No. of DCCV	2.1 ± 0.9	1.6 ± 0.7	0.58
LAA baseline AFCL, ms	147 ± 10	182 ± 16	**0.01**

Values are mean ± SD or n. **Bold** p values indicate significance ($p < 0.05$).

AFCL = atrial fibrillation cycle length; DCCV = direct current cardioversion; DE = delayed enhancement, LAA = left atrial appendage; other abbreviations as in Table 1.

frequently observed at dense DE regions than other sites: 68% of recorded Egms at dense DE sites showed organized activity versus 54% of Egms at patchy DE ($p < 0.0001$) and 47% of Egms at non-DE sites ($p < 0.0001$) (Fig. 6B).

MEAN EGM VOLTAGE DURING AF AT DENSE DE VERSUS PATCHY DE VERSUS NON-DE SITES. The global mean bipolar Egm voltage during AF (8-s recording period) was 0.78 ± 0.89 mV. Egms at dense DE areas had significantly lower mean bipolar voltage (0.63 ± 0.8 mV) than those at patchy DE areas (0.86 ± 1.09 mV, $p < 0.0001$) and non-DE regions (0.86 ± 0.89 mV, $p < 0.0001$) (Fig. 6C). There was no significant difference in bipolar Egm voltage at patchy DE versus non-DE regions ($p = 0.94$).

AF ablation results. Continuous CFAE ablation (at CFEmean <80 ms) prolonged AF CL within the LAA in 7 of 11 patients (64%) with long-persistent AF from a mean of 135 ms to 190 ms ($p < 0.05$). AF terminated in atrial tachycardia during CFAE ablation in 2 of 11 patients. Atrial tachycardias (1 roof dependent and 1 perimitral flutter) converted to sinus rhythm during linear ablation. CFAE ablation within the right atrium was necessary in 2 patients and resulted in prolongation of AF CL from a mean of 160 ms to 210 ms ($p < 0.05$). All long-persistent AF patients had linear ablations at the roof, mitral isthmus, and cavotricuspid isthmus. AF freedom was achieved in 64% (7/11) patients with long-persistant AF after a mean follow-up period of 18 ± 6 months and 1.7 procedures (range: 1 to 3).

Freedom from AF was achieved in 86% (6 of 7) of patients with persistent AF after a mean follow-up period of 18 ± 6 months and 1.1 procedures (range: 1 to 2).

Discussion

This study analyzes the relationship between atrial fibrosis and Egm characteristics (fractionation, CL, organization, and voltage) during human persistent AF. We provide correlation between the changing Egm characteristics during AF and the varying extent of atrial fibrosis. Our initial hypothesis was that DE areas (atrial fibrosis) would be associated with more chaotic and fractionated electrical activity. This study demonstrates the opposite. We found 2 different types of fibrosis pattern in the atrial wall, as depicted on high-resolution cardiac DE MRI: fibrosis in patients with persistent AF may be homogeneous/dense or patchy (i.e., nonconfluent) (Figs. 1 and 2). These aspects are associated with distinct electrical characteristics.

Validation of scar imaging by MRI. We used delayed gadolinium enhancement on high-resolution electrocardiography- and respiration-gated cardiac MRI with a reconstructed voxel size of 0.625 × 0.625 × 2.5 mm. As previously shown by Oakes et al. (13) using the same MRI sequence, regions of aDE correlated with regions of low voltage during sinus rhythm. The correlation between DE and fibrosis has been shown for ventricular scar (16) by histopathological studies and in very recent reports also for atrial tissue. We used the same slice-based voxel intensity analysis that was described by Oakes et al. (13) and Daccarett et al. (17) for aDE detection and segmentation (Fig. 1). To get even higher specificity for atrial fibrosis and reduce noise detection, we considered voxel intensities ≥4 SD of the mean in-plane voxel intensity, instead of 2 or 3 in the studies of Oakes et al. (13) and Daccarett et al. (17), to qualify for pathological DE (Fig. 1). There has been controversy about the ability of DE MRI to image scar in the thin-walled atrium. However, we do believe that the inverse correlation found in our study between DE and CFAE validates scar imaging. If the segmentation of aDE areas was incorrect, no correlation with electrical activity would have been observed.

As expected, this study demonstrates that the patients with long-persistent AF have a larger left atrium with a greater extent of aDE, a larger continuous CFAE area, and a shorter AF CL than those with persistent AF (Fig. 4A). Patients with very short LAA CL (<145 ms) were found to have a greater extent of total aDE (35% to 40% of LA surface) than patients with longer baseline AF CL (>170 ms) (Fig. 4B). Moreover, a negative correlation between the extent of aDE and baseline AF CL ($r = -0.74$; $p = 0.001$) (Fig. 4C) was found. These results demonstrate that the higher complexity of the fibrillating mechanisms/AF drivers in patients with long-persistent AF is associated with a greater extent of atrial fibrosis (aDE), suggesting that fibrosis and electrical complexity increase in parallel with the duration of uninterrupted AF as the consequences of remodeling.

Spatial distribution of dense/continuous aDE and patchy DE. Dense DE was consistently encountered on the left side of the posterior LA (adjacent to the left PV ostia and within the track/path of the descending aorta) in all patients (Figs. 1C and 2). The predominance of fibrotic remodeling of the posterior LA was recently reported using post-mortem histological analysis of the left atrium in patients with mitral valve AF (11). The consistent presence of dense DE in the left-sided posterior LA wall in all our patients may suggest higher shear/stretch forces in this region of the left atrium. Patchy DE was observed at the right posterior LA, LA roof, and anteroseptal LA wall.

CFAE, aDE, and ablation strategy. Our results demonstrate that a majority (48%) of continuous CFAE sites are not related to DE areas and occur at healthy atrial tissue (non-DE) without evidence of fibrosis on MRI. However, we found that 41% of continuous CFAE sites occur at patchy DE sites, with a lower content (37 ± 12%) of DE compared with dense DE regions with a higher DE content (96 ± 4% regional enhancement). With the exception of organized electrical activity, which was observed more often at patchy DE regions than at non-DE sites, no significant electrical differences were notable between patchy DE and non-DE sites. However, 19 ± 6% of CFAE sites do occur at border zones of or within the dense DE regions. This finding may be of importance. Ablative treatment of AF is more difficult in long-persistent AF, especially when the

baseline AF CL is <150 ms (18). In these patients, isolation of PVs needs to be followed by CFAE ablation and linear lesions to obtain higher rates of freedom from acute and long-term arrhythmia. It was recently shown that the ablation of continuous CFAE sites in persistent AF is associated with AF CL prolongation in ~50% of ablation attempts (15). Importantly, in our current study, we found that 41% of continuous CFAE sites occurred at patchy DE areas, 11% of CFAE at dense DE areas, and 48% of CFAE at healthy non-DE atrial regions. A recent study with high-density mapping of AF revealed higher bipolar voltage values at CFAE sites than at LA sites without CFAE, confirming our findings of an inverse relationship between CFAE and atrial fibrosis (DE) (8). In fact, recent studies have shown that at least 50% of CFAE sites are passive bystanders (e.g., due to nonlocal signals or wave collisions) (8,19). This study confirms that most continuous CFAE sites occur at healthy atrial sites. Thus, our results suggest that during CFAE ablation, we mostly target healthy (non-DE or patchy DE) tissue rather than fibrotic (dense DE) areas. Therefore, these data may be of clinical importance for the AF ablationist. Because of the limited specificity of CFAE sites as arrhythmia substrate in AF (only 50% of continuous CFAE sites will have an impact on AF CL during ablation [15]) and most CFAE regions being healthy atrial tissue (without or with little evidence of fibrosis), CFAE ablation should be limited to regions where further linear ablation may be needed (LA roof, inferior left atrium facing the CS, mitral isthmus region, and other cardiac veins such as the CS) and to the atrial sites with rapid activity and local activation gradients. The present study used post-processing for the initially time-consuming magnetic resonance image processing (detection/segmentation of DE) for comparison with continuous CFAE sites. Therefore, we did not compare the impact of ablation at specific CFAE sites (dense vs. patchy DE regions) on AF CL or AF termination. However, we did ablate continuous CFAE sites in all 11 patients with long-persistent AF, which significantly prolonged AF CL (from a mean of 135 to 190 ms) ($p < 0.05$) in 7 of 11 (64%) patients with long-persistent AF.

CFAE in AF. The impact of atrial fibrosis on wave propagation has been studied in animal models of persistent AF (12). With disease progression (short-persistent to long-persistent AF), it may be likely that an increasing amount of fibrosis (DE) within the atrial wall allows formation of a substrate favorable for slow conduction and re-entry of wavelets capable of perpetuating AF. We observed that the patients with long-persistent AF and a shorter AF CL had a greater extent of aDE than patients with persistent AF and longer AF CL. Although dense DE sites display Egms with lower voltage and slower CL instead of continuous CFAE, they may be important arrhythmia contributors in long-persistent AF. Dense DE regions may participate in perpetuating the arrhythmia by acting as boundaries critical to anchor rotors or transient re-entrant circuits. Alternatively, the re-entrant circuits may occur within or around the fibrotic areas.

Recently, simultaneous high-density endo- and epicardial mapping in human AF has shown dissociated/dyssynchronous activation of LA endo- and epicardium with distinct sites of breakthrough (20). The endo-/epicardial dissociation and dyssynchronous activation may also contribute to CFAE generation during AF. Our observation of more regular and nonfractionated electrical activity at dense DE regions may be explained by the absence of multiple layers of atrial muscle in dense DE regions. The CFAE within patchy DE and dense DE atrial regions may be the consequence of fibrosis-related slow conduction and/or endocardial/epicardial dyssynchronous activity. Therefore, one can hypothesize that the CFAE sites in or around dense scar may represent preferential ablation targets in patients with persistent AF. Further studies would be needed to demonstrate that ablation targeting CFAE sites in or around dense scar allows for a more specific treatment of persistent AF.

Study limitations. DE-MRI RESOLUTION. The thickness of the LA wall varies from 1 to 7 mm. LA regions with wall thickness of 1 mm are below the resolution of currently used MRI. With further advances in MRI-based fibrosis imaging (use of higher magnetic field gradients [3-T instead of 1.5-T] with a better signal-to-noise ratio and T1-T2 imaging), it would be interesting to assess the transmurality of atrial fibrosis.

Dense DE areas were electrically distinct from patchy DE or non-DE LA sites. However, mapping with a 20-pole catheter (1-mm electrodes, 4-mm spacing), we could not electrically distinguish (with the exception of Egm organization) (Fig. 6B) between patchy DE regions and non-DE areas. High-resolution, simultaneous whole-chamber mapping with more advanced mapping tools may allow a deeper and better understanding of wave propagation during AF and the impact of atrial fibrosis on proarrhythmia.

MRI resolution for fibrosis detection is limited. It is possible that patchy DE sites with intermittent DE may partly be due to MRI "noise" detection. In that case, some of the patchy DE sites might even be healthier and not contain any fibrosis.

Conclusions

Using high-resolution, late-enhanced MRI for atrial fibrosis imaging and high-density mapping during AF, we found most (48%) of the continuous CFAE sites at LA regions without any DE and 41% of CFAE at regions with less DE (patchy DE). Most (78%) of the dense DE sites did not display CFAE but rather low-voltage electrical activity. However, 19% of CFAE occur within or around dense DE sites. These findings may be of clinical importance for choosing the ablation strategy in patients with persistent AF. The region of slow conduction (with fractionated or rapid activity) within or around the areas of atrial fibrosis may be a promising ablation target in patients with persistent AF. Alternatively, novel global biatrial mapping systems are currently in the clinical evaluation phase and will allow for

a more mechanistically oriented ablation strategy in persistent AF that targets the patient-specific AF sources and drivers (21–23).

Reprint requests and correspondence: Dr. Amir S. Jadidi, Hôpital Cardiologique du Haut-Lévêque, 33604 Bordeaux-Pessac, France. E-mail: amir.s.jadidi@gmail.com.

REFERENCES

1. Haissaguerre M, Jais P, Shah DC, et al. Spontaneous initiation of atrial fibrillation by ectopic beats originating in the pulmonary veins. N Engl J Med 1998;339:659–66.
2. Jais P, Haissaguerre M, Shah DC, et al. Regional disparities of endocardial atrial activation in paroxysmal atrial fibrillation. Pacing Clin Electrophysiol 1996;19:1998–2003.
3. Nademanee K, McKenzie J, Kosar E, et al. A new approach for catheter ablation of atrial fibrillation: mapping of the electrophysiologic substrate. J Am Coll Cardiol 2004;43:2044–53.
4. de Bakker JM, Wittkampf FH. The pathophysiologic basis of fractionated and complex electrograms and the impact of recording techniques on their detection and interpretation. Circ Arrhythm Electrophysiol 2010;3:204–13.
5. Spach MS, Heidlage JF, Dolber PC, et al. Mechanism of origin of conduction disturbances in aging human atrial bundles: experimental and model study. Heart Rhythm 2007;4:175–5.
6. Kawara T, Derksen R, de Groot JR, et al. Activation delay after premature stimulation in chronically diseased human myocardium relates to the architecture of interstitial fibrosis. Circulation 2001;104:3069–75.
7. Konings KT, Kirchhof CJ, Smeets JR, et al. High-density mapping of electrically induced atrial fibrillation in humans. Circulation 1994;89:1665–80.
8. Jadidi AS, Duncan E, Miyazaki S, et al. Functional nature of electrogram fractionation demonstrated by left atrial high-density mapping. Circ Arrhythm Electrophysiol 2012;5:32–42.
9. Zlochiver S, Yamazaki M, Kalifa J, et al. Rotor meandering contributes to irregularity in electrograms during atrial fibrillation. Heart Rhythm 2008;5:846–54.
10. Lin J, Scherlag BJ, Zhou J, et al. Autonomic mechanism to explain complex fractionated atrial electrograms. J Cardiovasc Electrophysiol 2007;18:1197–205.
11. Corradi D, Callegari S, Benussi S, et al. Myocyte changes and their left atrial distribution in patients with chronic atrial fibrillation related to mitral valve disease. Hum Pathol 2005;36:1080–9.
12. Tanaka K, Zlochiver S, Vikstrom KL, et al. Spatial distribution of fibrosis governs fibrillation wave dynamics in the posterior left atrium during heart failure. Circ Res 2007;101:839–47.
13. Oakes RS, Badger TJ, Kholmovski EG, et al. Detection and quantification of left atrial structural remodeling with delayed-enhancement magnetic resonance imaging in patients with atrial fibrillation. Circulation 2009;119:1758–67.
14. Tsai WC, Lin YJ, Tsao HM, et al. The optimal automatic algorithm for the mapping of complex fractionated atrial electrograms in patients with atrial fibrillation. J Cardiovasc Electrophysiol 2009;21:21–6.
15. Takahashi Y, O'Neill MD, Hocini M, et al. Characterization of electrograms associated with termination of chronic atrial fibrillation by catheter ablation. J Am Coll Cardiol 2008;51:1003–10.
16. Wijnmaalen AP, van der Geest RJ, van Huls van Taxis CF, et al. Head-to-head comparison of contrast-enhanced magnetic resonance imaging and electroanatomical voltage mapping to assess post-infarct scar characteristics in patients with VTs: real-time image integration and reversed registration. Eur Heart J 2011;32:104–14.
17. Daccarett M, Badger TJ, Akoum N, et al. Association of left atrial fibrosis detected by delayed-enhancement magnetic resonance imaging and the risk of stroke in patients with atrial fibrillation. J Am Coll Cardiol 2011;57:831–8.
18. Haissaguerre M, Lim KT, Jacquemet V, et al. Atrial fibrillatory cycle length: computer simulation and potential clinical importance. Europace 2007;9:64–70.
19. Narayan SM, Wright M, Derval N, et al. Classifying fractionated electrograms in human atrial fibrillation using monophasic action potentials and activation mapping: evidence for localized drivers, rate acceleration, and nonlocal signal etiologies. Heart Rhythm 2011;8:244–53.
20. Allessie MA, de Groot NM, Houben RP, et al. Electropathological substrate of long-standing persistent atrial fibrillation in patients with structural heart disease: longitudinal dissociation. Circ Arrhythm Electrophysiol 2010;3:606–15.
21. Cuculich PS, Wang Y, Lindsay BD, et al. Noninvasive characterization of epicardial activation in humans with diverse atrial fibrillation patterns. Circulation 2010;122:1364–72.
22. Narayan SM, Krummen DE, Shivkumar K, et al. CONFIRM (Conventional Ablation for Atrial Fibrillation With or Without Focal Impulse and Rotor Modulation) Trial. J Am Coll Cardiol 2012;60:628–36.
23. Haissaguerre M, Hocini M, Shah A, et al. Noninvasive panoramic mapping of human atrial fibrillation mechanisms: a feasibility report. J Cardiovasc Electrophysiol 2013;24:711–7.

Key Words: ablation ■ atrial delayed enhancement ■ atrial fibrillation ■ atrial fibrosis ■ complex fractionated atrial electrogram ■ cycle length ■ MRI ■ pulmonary vein isolation.

APPENDIX

For a supplemental figures, please see the online version of this article.